Clinical Infectious Diseases

MAJOR ARTICLE

In Vitro Antiviral Activity and Projection of Optimized Dosing Design of Hydroxychloroquine for the Treatment of Severe Acute Respiratory Syndrome Coronavirus 2 (SARS-CoV-2)

Xueting Yao,[1,a] Fei Ye,[2,a] Miao Zhang,[1,a] Cheng Cui,[1,a] Baoying Huang,[2,a] Peihua Niu,[2] Xu Liu,[1] Li Zhao,[2] Erdan Dong,[3] Chunli Song,[4] Siyan Zhan,[5] Roujian Lu,[2] Haiyan Li,[1,3,b] Wenjie Tan,[2,b] and Dongyang Liu[1,b]

[1]Drug Clinical Trial Center, Peking University Third Hospital, Beijing, China, [2]NHC Key Laboratory of Biosafety, National Institute for Viral Disease Control and Prevention, Chinese Center for Disease Control and Prevention, Beijing, China, [3]Department of Cardiology and Institute of Vascular Medicine, Peking University Third Hospital, Beijing, China, [4]Department of Orthopedics, Peking University Third Hospital, Beijing, China, and [5]Research Center of Clinical Epidemiology, Peking University Third Hospital, Beijing, China

Background. The severe acute respiratory syndrome coronavirus 2 (SARS-CoV-2) first broke out in 2019 and subsequently spread worldwide. Chloroquine has been sporadically used in treating SARS-CoV-2 infection. Hydroxychloroquine shares the same mechanism of action as chloroquine, but its more tolerable safety profile makes it the preferred drug to treat malaria and autoimmune conditions. We propose that the immunomodulatory effect of hydroxychloroquine also may be useful in controlling the cytokine storm that occurs late phase in critically ill patients with SARS-CoV-2. Currently, there is no evidence to support the use of hydroxychloroquine in SARS-CoV-2 infection.

Methods. The pharmacological activity of chloroquine and hydroxychloroquine was tested using SARS-CoV-2–infected Vero cells. Physiologically based pharmacokinetic (PBPK) models were implemented for both drugs separately by integrating their in vitro data. Using the PBPK models, hydroxychloroquine concentrations in lung fluid were simulated under 5 different dosing regimens to explore the most effective regimen while considering the drug's safety profile.

Results. Hydroxychloroquine (EC_{50} = 0.72 μM) was found to be more potent than chloroquine (EC_{50} = 5.47 μM) in vitro. Based on PBPK models results, a loading dose of 400 mg twice daily of hydroxychloroquine sulfate given orally, followed by a maintenance dose of 200 mg given twice daily for 4 days is recommended for SARS-CoV-2 infection, as it reached 3 times the potency of chloroquine phosphate when given 500 mg twice daily 5 days in advance.

Conclusions. Hydroxychloroquine was found to be more potent than chloroquine to inhibit SARS-CoV-2 in vitro.

Keywords. chloroquine; hydroxychloroquine; SARS-CoV-2.

In December 2019 the outbreak of a novel coronavirus, severe acute respiratory syndrome coronavirus 2 (SARS-CoV-2 or COVID-2019), was first reported in Wuhan, China. The outbreak has since rapidly spread to other provinces in mainland China, as well as other countries around the world. Currently, the number of people diagnosed with SARS-CoV-2 infection is increasing by approximately 1000 cases per day. Unfortunately, to date, no drugs have been approved by regulatory agencies for the treatment of SARS-CoV-2 infection.

Chloroquine is a widely used antimalarial with immunomodulatory effects [1–5]. In a recent in vitro study chloroquine was found to inhibit the growth of SARS-CoV-2 in vitro [6]. This finding has been supported by clinical studies conducted in approximately 100 patients with SARS-CoV-2 [7, 8].

Hydroxychloroquine is an analog of chloroquine that has fewer concerns about drug–drug interactions. In the previous SARS outbreak, hydroxychloroquine was reported to have anti–SARS-CoV activity in vitro [9]. This suggests that hydroxychloroquine may be a potential pharmacological agent for the treatment of COVID-19 infection. However, to date, there is no clinical evidence to support the use of hydroxychloroquine as a treatment for SARS-CoV-2 infection.

The molecular mechanism of action of chloroquine and hydroxychloroquine has not been fully elucidated. Findings from previous studies have suggested that chloroquine and hydroxychloroquine may inhibit the coronavirus through a series of steps. First, the drugs can change the pH at the surface of the cell membrane and, thus, inhibit the fusion of the virus to

Received 25 February 2020; editorial decision 2 March 2020; accepted 12 March 2020; published online March 9, 2020.

[a]X. Y., F. Y., M. Z., C. C., and B. H. contributed equally to this work.

[b]D. L., W. T., and H. L. contributed equally to this work.

Correspondence: D. Liu, Drug Clinical Trial Center, Peking University Third Hospital, 49 Huayuan North Rd, Haidian District, Beijing 100089, China (liudongyang@sina.vip.com).

Clinical Infectious Diseases® 2020;71(15):732–9

DOI: 10.1093/cid/ciaa237

the cell membrane. It can also inhibit nucleic acid replication, glycosylation of viral proteins, virus assembly, new virus particle transport, virus release, and other processes to achieve its antiviral effects [10].

A reliable estimation of hydroxychloroquine and chloroquine concentrations in the lung, the target tissue, may be used for guiding dose recommendations. Physiologically based pharmacokinetic (PBPK) models are a mathematical modeling technique that can predict drug concentrations in human tissues in silico by integrating physiological and drug disposition parameters. PBPK models are widely used in drug development to help identify whether a clinical trial is warranted as well as help guide the use of drugs based on predictions from well-validated models [11, 12].

In this study we aimed to (1) investigate the antiviral and prophylactic activity of hydroxychloroquine and chloroquine in vitro, (2) build a PBPK model for hydroxychloroquine and chloroquine using data from the literature, and (3) predict drug concentrations under different dosing regimens using the developed PBPK models.

METHODS

In Vitro Antiviral Activity Experiment

Experiment Materials

Chloroquine phosphate and hydroxychloroquine sulfate were purchased from Beijing Innochem Science & Technology Co, Ltd. The lyophilized powder was diluted in double-distilled water to 10 mM. Hydroxychloroquine sulfate was readily soluble in water. Chloroquine phosphate was dissolved by shaking the solution at room temperature for 2 hours. The chloroquine and hydroxychloroquine solutions were filtered through a 0.22-μm membrane and were then stored at − 80°C. The clinically isolated SARS-CoV-2 virus strain, C-Tan-nCoV Wuhan strain 01, was propagated in Vero cells.

Cell Culture

The Vero cells were derived from the African green monkey kidney and were grown in Dulbecco's Modified Eagle Medium (DMEM; Sigma Aldrich, Boston, MA) supplemented with 5% fetal bovine serum (HyClone, Logan, UT). The cells were maintained in a humidified atmosphere with 5% CO_2 at 37°C. The culture medium was replaced each day.

Antiviral Activity Assay

The anti–SARS-CoV-2 activity of chloroquine and hydroxychloroquine was investigated in vitro. Cells were seeded into 96-well plates at a density of 1×10^4 cells/well and were grown for 24 hours. The in vitro experiment was divided into 2 sections, as follows: (1) the treatment study and (2) the prophylactic study.

Treatment Study

In the treatment study Vero cells were infected at a multiplicity of infection (MOI) of 0.01 (100 plaque-forming units/well) for 2 hours at a temperature of 37°C.Virus input was washed with DMEM and the cells were then treated with medium containing either chloroquine or hydroxychloroquine at 0.032, 0.16, 0.80, 4, 20, or 100 μM for 24 or 48 hours.

Prophylactic Study

Vero cells were pretreated with chloroquine or hydroxychloroquine for 2 hours and then were removed from the drug-containing medium and washed by DMEM. The virus was then added to the infected Vero cells (as described for the treatment study) for 2 hours. Following this, the fresh drug-free medium was added and the cells were incubated for 24 or 48 hours.

The supernatant was collected, and, the RNA was extracted and analyzed by relative quantification using real-time reverse transcriptase–polymerase chain reaction (RT-PCR) (methods described in a previously published study) [13, 14].

Viral RNA Extraction and Reverse Transcriptase–Polymerase Chain Reaction

Viral RNA was extracted from 100 μL of supernatant of infected cells using the automated nucleic acid extraction system (Tianlong, China) and the manufacturer's instructions. Detection of the SARS-CoV-2 virus was performed using the One Step Prime Script RT-PCR kit (TaKaRa, Japan) on the Light Cycler 480 Real-Time PCR system (Roche, Rotkreuz, Switzerland) with primers. The following sequences were used:

forward primer: 5′-AGAAGATTGGTTAGATGATGATAGT-3′;
reverse primer:5′-TTCCATCTCTAATTGAGGTTGAACC-3′;
and probe:5′-FAM-TCCTCACTGCCGTCTTGTTG ACCA-BHQ1–3′.

All experiments were conducted in triplicates. The relative expression was estimated using the $2^{-\Delta\Delta Ct}$ method.

Statistical Analysis

A sigmoidal concentration-response function, Y = Bottom + (Top-Bottom)/ [1 + 10^([LogEC$_{50}$ − X] × HillSlope)], was fit to the data using nonlinear regression. The EC_{50} values were calculated using PRISM (GraphPad Software, San Diego, CA).

PBPK Model Development, Validation, and Simulation

The PBPK models for chloroquine and hydroxychloroquine were developed using the Simcyp simulator (version 18). The chloroquine compound file was provided by Simcyp Limited (a Certara company; Blades Enterprise Centre, Sheffield, UK), and the hydroxychloroquine compound file was self-built. Physical and chemical parameters were obtained from the literature [15]. Pharmacokinetic parameters, such as liver intrinsic clearance, the

fraction of dose entering the enterocytes (fa) and first-order absorption rate constant (ka), were determined from clinical data [16]. These data are summarized in Tables 1 and 2 in Supplement File 1. To further predict drug concentrations in lung fluid, we assumed perfusion limited tissue distribution and included an additional tissue compartment (other than default lung organ) in the model to represent lung tissue. This set up allowed us to use the lung to blood concentration ratio for chloroquine and hydroxychloroquine obtained from animal studies [17, 18].

Validation Data

Published chloroquine and hydroxychloroquine clinical trial data were used to validate the developed PBPK models (details summarized in Table 3 in Supplement File 2) [16, 19–23]. Data obtained from the literature in graphical form were extracted using Plot Digitizer (version 2.26, GetData). Pharmacokinetic parameters that could not be sourced from the literature were estimated using extracted data in Phoenix (version 8.6; Certara Company).

Validation Method

Concentration-time profiles were simulated under different published clinical trial protocols using the developed PBPK models for hydroxychloroquine and chloroquine [16, 19–23]. The Simcyp "Healthy volunteer," "Chinese healthy volunteer," and "Pediatric" virtual populations were used in the validation simulations as the reported clinical trials were conducted in Caucasian, Chinese, and children populations, respectively.

Simulated exposure data were compared with observed data. The criterion to determine model accuracy was based on whether the observed data fell within the 90% confidence interval of the predicted values. The ratio of predicted pharmacokinetic (PK) parameters (eg, the maximum concentration [C_{max}] and area under the curve [AUC]) to observed values was used to evaluate model performance. The predicted values were considered reasonable if the ratio of predicted to observed data was within a predefined 2-fold range ($0.5 \leq \text{ratio} \leq 2.0$).

Simulation Method

The exposure of chloroquine and hydroxychloroquine in the lung fluid (lung), plasma, and blood was simulated under different dosing regimens (shown in Table 1) using the validated PBPK models. A correction factor for chloroquine base and hydroxychloroquine base was input into the model simulations. Chloroquine phosphate 500 mg is equivalent to 300 mg of chloroquine base, and 200 mg of hydroxychloroquine sulfate is equivalent to 155 mg of hydroxychloroquine base. The "Chinese healthy volunteers" virtual population provided in Simcyp was used for the simulations. All simulations were performed with 10 trials and 10 subjects per trial. Virtual subjects were aged between 20 to 50 years of age, and 50% of the subjects were male and 50% female.

Dose Regimen Optimization

The PBPK models were used to predict the lung tissue concentrations of chloroquine and hydroxychloroquine under different dosing regimens (Table 1). The lung trough concentrations on days 1, 3, 5, and 10 were adjusted by the plasma unbound fraction ($f_{u,plasma}$) to obtain the free lung trough concentration. The ratio of the free lung trough concentration to the in vitro EC_{50} values (R_{LTEC}) was calculated and the results tabulated. In a recent clinical trial, 500 mg of chloroquine phosphate given twice daily was shown to be effective on study day 5 ($R_{LTEC, day5}$). This dosing regimen for chloroquine was used as the target for dose optimization for hydroxychloroquine (ie, the R_{LTEC} of hydroxychloroquine should not be lower than the $R_{LTEC, day5}$ of chloroquine at any time).

RESULTS

Antiviral Activity In Vitro

Results from the in vitro study showed that both chloroquine and hydroxychloroquine have good antiviral activity. Chloroquine and

Table 1. Ratios of Free Lung Tissue Trough Concentration/EC_{50} (R_{LTEC}) Under Different Dosage Regimens

		R_{LTEC}			
Drug and ID	Dosing Regimen	Day 1	Day 3	Day 5	Day 10
Chloroquine phosphate					
A.	D1–D10 500 mg BID	2.38	5.92	18.9	40.7
Hydroxychloroquine sulfate					
B.	D1 800 mg + 400 mg ; D2–D10 400 mg QD	33.3	55.1	103	168
C.	D1 600 mg BID ; D2–D10 400 mg QD	31.7	54.7	103	169
D.	D1 600 mg BID ; D2–D10 200 mg BID	31.7	53.1	101	167
E.	D1 400 mg BID ; D2–D10 200 mg BID	21.0	38.9	85.4	154
F.	D1 400 mg BID ; D2–D5 200 mg BID	21.0	38.9	85.4	83.3

Abbreviations: BID, twice daily; QD, once daily; R_{LTEC}, ratio of free lung tissue trough concentration/EC_{50}.

hydroxychloroquine were found to decrease the viral replication in a concentration-dependent manner. The EC_{50} values for chloroquine were 23.90 and 5.47 μM at 24 and 48 hours, respectively (Figure 1A). EC_{50} values for hydroxychloroquine were 6.14 and 0.72 μM at 24 and 48 hours, respectively (Figure 1B).

Antiviral Pretreatment Activity In Vitro

Hydroxychloroquine exhibited a superior in vitro antiviral effect in comparison to chloroquine when the drug was added prior to the viral challenge. The EC_{50} values for chloroquine were greater than 100 and 18.01 μM at 24 and 48 hours, respectively. EC_{50} values for hydroxychloroquine were 6.25 and 5.85 μM at 24 and 48 hours, respectively. It was noted that, with longer incubation times, the EC_{50} values for chloroquine and hydroxychloroquine tended to decrease. The inhibitory effect of chloroquine was poor. This was particularly evident at 24 hours whereby, even at the highest concentration of chloroquine used in the study, the inhibition rate did not exceed 50% (Figure 1C, D).

PBPK Model Development, Validation, and Simulation

Validation Results

The predicted and observed plasma/blood concentration time profiles for chloroquine and hydroxychloroquine are shown in Figure 2. Intravenous data were used to understand the distribution and elimination phase of the 2 drugs, and oral administration data were used to understand the intracorporal absorption process. Most of the observed data fell within the 90% prediction interval. The ratio of predicted to observed PK parameters (C_{max} and AUC) were within the range of 0.5 to 2.0 (details summarized in Table 4 in Supplement File 2), indicating that the prediction accuracy of the developed PBPK models was acceptable and could be used to simulate the different dosing scenarios.

Simulation Results

The simulated lung, blood, and plasma concentration time profiles for chloroquine and hydroxychloroquine under the different dosing regimens are shown in Figure 3. It can be seen that the lung, blood, and plasma concentrations of chloroquine increased slowly after the first dose was given and were yet to reach steady state on day 10. The simulated chloroquine concentration in lung tissue was much higher than in plasma, where the lung to plasma ratio increased with time and reached a ratio of approximately 400. The projected lung, blood, and plasma concentrations of hydroxychloroquine rapidly increased and reached steady state following the initial loading dose and subsequent maintenance doses (Figure 3B, C).

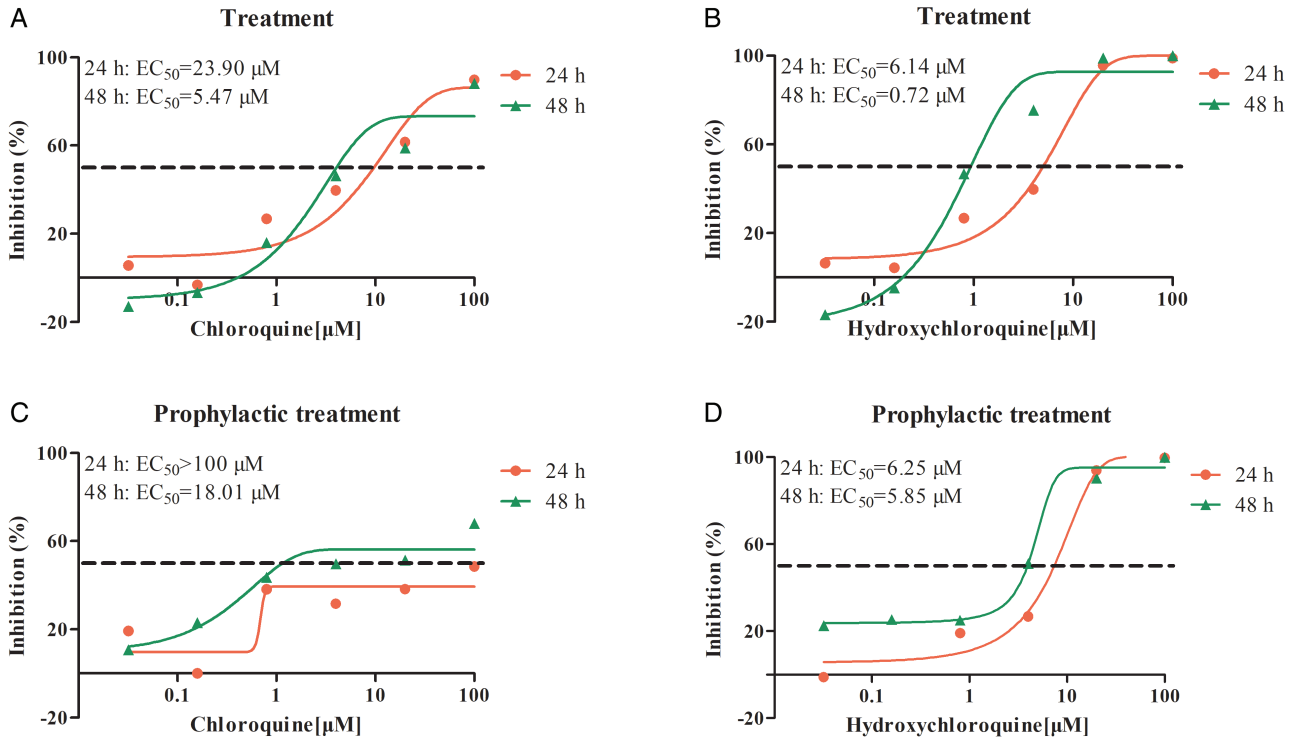

Figure 1. The antiviral activities of chloroquine and hydroxychloroquine for treatment or prophylactic treatment against SARS-CoV-2 in vitro. The antiviral activities of chloroquine and hydroxychloroquine for therapeutic and prophylactic use were tested on the Vero cells infected with a SARS-CoV-2 clinically isolated strain. *A* and *B*, For the treatment group, chloroquine and hydroxychloroquine were added to culture medium after the infection of Vero cells and cells were incubated for 24 or 48 hours. *C* and *D*, For the prophylactic treatment group, the Vero cells were pretreated with chloroquine and hydroxychloroquine for 2 hours, and then washed by medium. Virus was added to infect cells. After that, the fresh drug-free medium was added and cells were incubated for 24 or 48 hours. The viral yield in the cell supernatant was quantified by RT-PCR. Abbreviations: RT-PCR, reverse transcriptase–polymerase chain reaction; SARS-CoV-2, severe acute respiratory syndrome coronavirus 2.

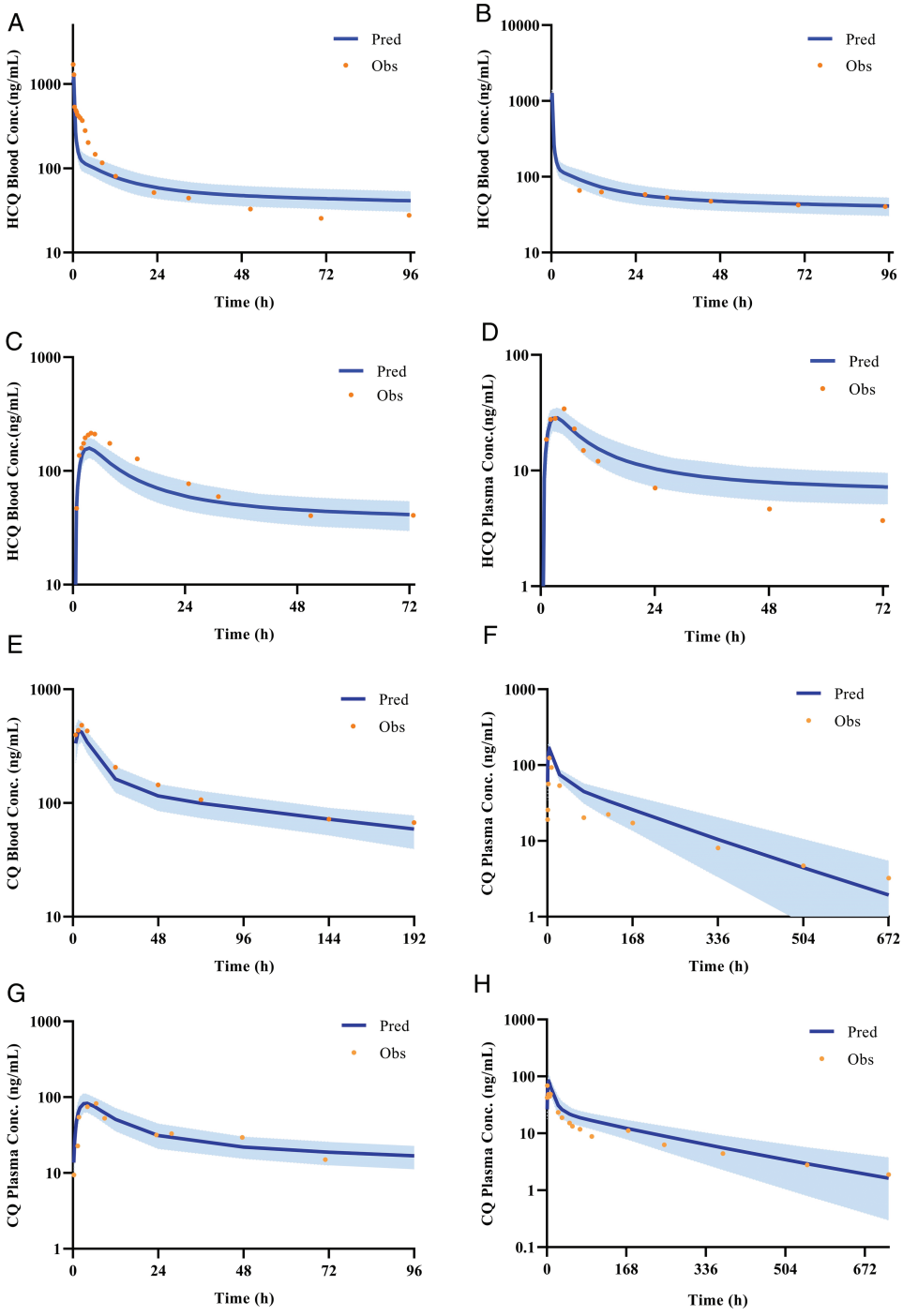

Figure 2. Predicted and observed mean arithmetic concentration profiles. *A* and *B*, Validation for HCQ PBPK model by blood data after intravenous administration, *C*, Validation for HCQ PBPK model by blood data after oral administration. *D*, Validation for HCQ PBPK model by plasma data after oral administration. *E*, Validation for CQ PBPK model by blood data after oral administration. *F*, Validation for CQ PBPK model by blood data after intravenous administration. *G*, Validation for CQ PBPK model by plasma data after oral administration. *H*, Validation for CQ PBPK model by plasma data after oral administration. Details are summarized in Tables 3 and 4 in Supplement File 2. Abbreviations: conc, concentration; CQ, chloroquine; HCQ, hydroxychloroquine; Obs, observed; PBPK, physiologically based pharmacokinetic; Pred, predicted.

Suggested Dosing Regimens for Hydroxychloroquine to Treat SARS-CoV-2 Infection

The free lung trough concentrations were also projected from the simulations. The R_{LTEC} under the different dosing regimens is shown in Table 1. The R_{LTEC} values of hydroxychloroquine were found to be higher than the R_{LTEC} values of chloroquine on days 1, 3, 5, and 10. This suggests that hydroxychloroquine may achieve ideal clinical efficacy under the simulated dosing regimens.

The R_{LTEC} on day 1 was notably higher for hydroxychloroquine than for chloroquine. This is likely due to the loading dose of

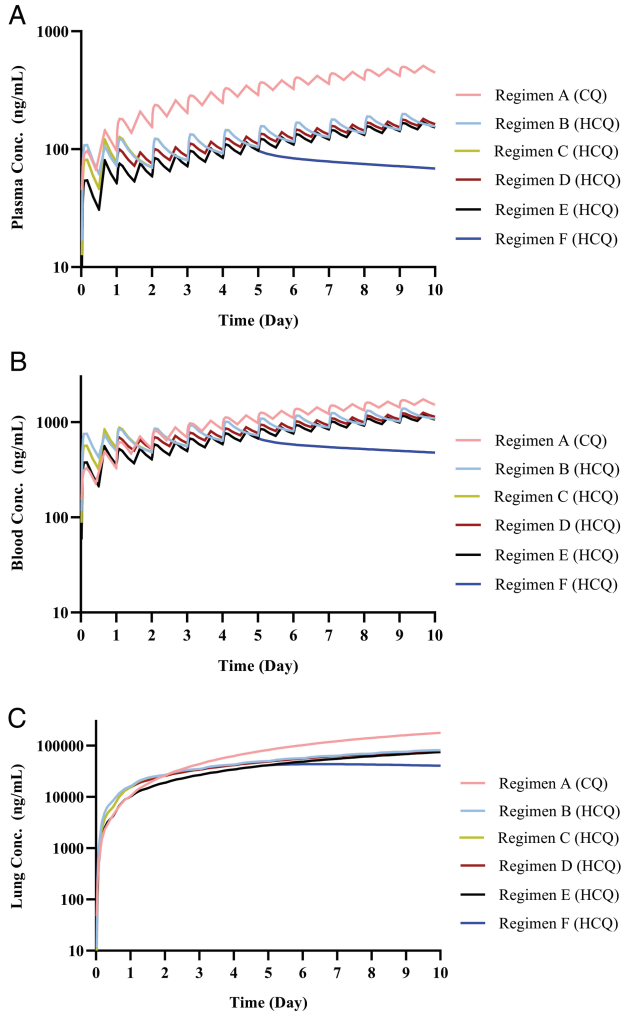

Figure 3. Predicted plasma (*A*), blood (*B*), and lung (*C*) concentration–time profiles of CQ under the dose regimen A, and HCQ under dose regimen B, regimen C, regimen D, regimen E, and regimen F. Lung tissue concentrations were predicted based on animal data (see Methods). Abbreviations: conc, concentration; CQ, chloroquine; HCQ, hydroxychloroquine.

hydroxychloroquine given, thus enabling a faster clinical effect. There was no significant difference between the once- and twice-daily maintenance dosing regimens (regimen C and D, respectively) when used from day 2 to day 10; hence, the once-daily dosing regimen may be preferred to improve patient compliance. Despite regimen F being a 5-day treatment regimen, the lung trough concentrations were still above the target concentration on day 10. However, if the treatment duration of regimen F was extended to 10 days (ie, regimen E), it resulted in a higher drug concentration on day 10. Overall, regimen F may be the best regimen while considering both efficacy, safety, and patient compliance. These simulations were used to provide timely support on proper dose selection of CQ and HCQ in a clinical study commenced in February, 2020 in Wuhan City (http://www.chictr.org.cn/showproj.aspx?proj=49482).

DISCUSSION

In this study, hydroxychloroquine exhibited better in vitro anti–SARS-CoV-2 activity than chloroquine. This was demonstrated by the EC_{50} values for hydroxychloroquine always being smaller than the EC_{50} values for chloroquine, indicating that hydroxychloroquine has a more potent antiviral activity (shown in Figure 1). In the study by Wang et al [6], chloroquine was shown to have an inhibitory effect on SARS-CoV-2 with an EC_{50} value of 1.13 μM after a 48-hour incubation time. These findings are comparable to our in vitro chloroquine results of an EC_{50} value of 5.47 μM. In addition, an unpublished clinical trial has demonstrated the therapeutic effect of chloroquine in patients with SARS-CoV-2. On the basis of hydroxychloroquine's superior antiviral and prophylactic activity, as well as its more tolerable safety profile in comparison to chloroquine, we believe that hydroxychloroquine may be a promising drug for the treatment of SARS-CoV-2 infection [24].

In our study we noted that the EC_{50} values for hydroxychloroquine and chloroquine decreased with longer incubation times. This suggests that incubation time may influence the drug's antiviral activity. Both hydroxychloroquine and chloroquine have been reported to accumulate in cells [25]. It is possible that a longer incubation time may provide more time for the drug to accumulate to higher intracellular concentrations and ultimately exhibit a better antiviral effect [26]. Another possible explanation is that the drug-induced cytotoxicity may take time to develop, and hence, the drug effect may increase with time [27].

The PBPK model for hydroxychloroquine and chloroquine was validated with in vivo PK data from humans, with predictions of lung tissue drug concentrations supported by findings in rats and mice. A high lung to plasma partition coefficient ratio (Kp ratio) reported in animal studies was used to imitate the drugs' high accumulation in lung tissue. The Kp ratio of both drugs for humans was assumed to be same as the ratio for chloroquine in rats because there were no human data available. This assumption may be reasonable as the transportation of both drugs is completely via passive diffusion (ie, no transporters are involved). Further cell and animal researches are underway to update these PBPK models (manuscripts in preparation).

In some patients it has been reported that their immune response to the SARS-CoV-2 virus results in an increase of cytokines interleukin (IL)-6 and IL-10 [13, 28]. This may progress to a cytokine storm, followed by multiorgan failure and potentially death. Both hydroxychloroquine and chloroquine have immunomodulatory effects and can suppress the increase of immune factors [29, 30]. Bearing this in mind, it is possible that early treatment with either of the drugs may help prevent the progression of the disease to a critical, life-threatening state. In critically ill patients with SARS-CoV-2 the use of corticosteroids may be harmful [31]; however, the use

of immunosuppressants (eg, tocilizumab) is not ideal either as they can suppress the immune system and lead to an increased risk of infection [32]. In this setting, hydroxychloroquine may be an ideal drug to treat SARS-CoV-2 infection as it can inhibit the virus via its antiviral effects and help mediate the cytokine storm via its immunomodulatory effects. Based on work conducted in our laboratory, we recommend the concomitant use of low-dose hydroxychloroquine with an anti-inflammatory drug to help mitigate the cytokine storm in critically ill patients with SARS-CoV-2.

Several clinical trials are currently investigating the use of hydroxychloroquine to treat SARS-CoV-2 infection. However, it is worth noting that the dosing regimens used in these trials are mainly based on previous clinical experience, raising the concern that adverse effects may occur in study participants (The dose regimen of chloroquine phosphate and hydroxychloroquine sulfate from registered clinical trials were summarized in Supplement File 3). In this study, an optimized dosing regimen was designed for hydroxychloroquine to have a high loading dose and low maintenance dose based on its unique pharmacokinetics (ie, high accumulation in cells and long elimination half-life). Using PBPK modeling and simulation techniques the optimal dosing regimen for hydroxychloroquine was evaluated *in silico*. The simulation results demonstrated that regimen F was able to achieve treatment efficacy as well as have a good safety profile, even considering possible underestimation of drug efficacy to some extent. However, future clinical trials evaluating this regimen are required before it can be widely used to treat COVID-19. The combination of the in vitro antiviral activity data and predicted drug concentrations in this study is being used to support the design of dosing regimens used in a clinical study in COVID-19 patients (http://www.chictr.org.cn/showproj.aspx?proj=49482).

Supplementary Data

Supplementary materials are available at *Clinical Infectious Diseases* online. Consisting of data provided by the authors to benefit the reader, the posted materials are not copyedited and are the sole responsibility of the authors, so questions or comments should be addressed to the corresponding author.

Notes

Acknowledgments. The authors thank Dr Lisa Almond, Alice Ke, Mian Zhang and Luke Guilliatt from Simcyp Limited for providing the chloroquine compound file. The authors would also like to thank Dr. Isabelle Hui-San Kuan and Dr. Xiao Zhu of New Zealand and Dr. Ping Zhao of the Bill & Melinda Gates Foundation for their proofreading work. At the same time, authors would also like to thank Dr. Gaohua Lu of GlaxoSmithKline UK, who guided the optimization of the PBPK model.

Author contributions. D. L. and H. L. conceived and designed the study. X. Y. designed and W. T., F. Y., B. H., P. N., L. Z., and R. L. conducted the experiments of in vitro antiviral activity. X. L. analyzed the experiment data. X. Y. and M. Z. developed and optimized the chloroquine and hydroxychloroquine PBPK model. C. C. designed the dose regiments of hydroxychloroquine. X. Y., M. Z., C. C., X. L., and D. L. prepared this manuscript. H. L., E. D., C. S., S. Z., and W. T. reviewed this manuscript.

Financial support. This work was supported by the "13th Five-Year" National Major New Drug Projects of China, Ministry of Science and Technology of the People's Republic of China (grant number 2017ZX09101001–002–001) and the Bill & Melinda Gates Foundation (grant number OPP1204780).

Potential conflicts of interest. C. S., H. L., and D. L. have patents pending for antimicrobial infection pharmoceutical composition and its application. All other authors report no potential conflicts. All authors have submitted the ICMJE Form for Disclosure of Potential Conflicts of Interest. Conflicts that the editors consider relevant to the content of the manuscript have been disclosed.

References

1. Romanelli F, Smith KM, Hoven AD. Chloroquine and hydroxychloroquine as inhibitors of human immunodeficiency virus (HIV-1) activity. Curr Pharm Des **2004**; 10:2643–8.
2. Keyaerts E, Vijgen L, Maes P, Neyts J, Van Ranst M. In vitro inhibition of severe acute respiratory syndrome coronavirus by chloroquine. Biochem Biophys Res Commun **2004**; 323:264–8.
3. Vincent MJ, Bergeron E, Benjannet S, et al. Chloroquine is a potent inhibitor of SARS coronavirus infection and spread. Virol J **2005**; 2:69.
4. Ooi EE, Chew JS, Loh JP, Chua RC. In vitro inhibition of human influenza A virus replication by chloroquine. Virol J **2006**; 3:39.
5. Li C, Zhu X, Ji X, et al. Chloroquine, a FDA-approved drug, prevents zika virus infection and its associated congenital microcephaly in mice. EBioMedicine **2017**; 24:189–94.
6. Wang M, Cao R, Zhang L, et al. Remdesivir and chloroquine effectively inhibit the recently emerged novel coronavirus (2019-nCoV) in vitro. Cell Res **2020**; 30:269–71.
7. Huang J. Efficacy of chloroquine and lopinavir/ ritonavir in mild/general novel coronavirus (CoVID-19) infections: a prospective, open-label, multicenter randomized controlled clinical study. Available at: http://www.chictr.org.cn/showproj.aspx?proj=49263. Accessed 13 February 2020.
8. Li Y. Ministry of Science and Technology of China: chloroquine phosphate is effective in the treatment of novel coronavirus pneumonia. Available at: http://news.ynet.com/2020/02/17/2388070t70.html. Accessed 17 February 2020.
9. Biot C, Daher W, Chavain N, et al. Design and synthesis of hydroxyferroquine derivatives with antimalarial and antiviral activities. J Med Chem **2006**; 49:2845–9.
10. Fox RI. Mechanism of action of hydroxychloroquine as an antirheumatic drug. Semin Arthritis Rheum **1993**; 23:82–91.
11. Food and Drug Administration. Physiologically based pharmacokinetic analyses-format and content guidance for industry. August 2018. Available at: https://www.fda.gov/media/101469/download. Accessed 17 February 2020.
12. Hsueh CH, Hsu V, Pan Y, Zhao P. Predictive performance of physiologically-based pharmacokinetic models in predicting drug-drug interactions involving enzyme modulation. Clin Pharmacokinet **2018**; 57:1337–46.
13. Huang C, Wang Y, Li X, et al. Clinical features of patients infected with 2019 novel coronavirus in Wuhan, China. Lancet **2020**; 395:497–506.
14. Zhu N, Zhang D, Wang W, et al. A novel coronavirus from patients with pneumonia in China, 2019. N Engl J Med **2020**; 382:727–33.
15. Collins KP, Jackson KM, Gustafson DL. Hydroxychloroquine: a physiologically-based pharmacokinetic model in the context of cancer-related autophagy modulation. J Pharmacol Exp Ther **2018**; 365:447–59.
16. Tett SE, Cutler DJ, Day RO, Brown KF. Bioavailability of hydroxychloroquine tablets in healthy volunteers. Br J Clin Pharmacol **1989**; 27:771–9.
17. Adelusi SA, Salako LA. Kinetics of the distribution and elimination of chloroquine in the rat. Gen Pharmacol **1982**; 13:433–7.
18. McChesney EW. Animal toxicity and pharmacokinetics of hydroxychloroquine sulfate. Am J Med **1983**; 75:11–8.
19. Fan HW, Ma ZX, Chen J, Yang XY, Cheng JL, Li YB. Pharmacokinetics and bioequivalence study of hydroxychloroquine sulfate tablets in Chinese healthy volunteers by LC-MS/MS. Rheumatol Ther **2015**; 2:183–95.
20. Tett SE, Cutler DJ, Day RO, Brown KF. A dose-ranging study of the pharmacokinetics of hydroxy-chloroquine following intravenous administration to healthy volunteers. Br J Clin Pharmacol **1988**; 26:303–13.
21. Walker O, Dawodu AH, Salako LA, Alván G, Johnson AO. Single dose disposition of chloroquine in kwashiorkor and normal children—evidence for decreased absorption in kwashiorkor. Br J Clin Pharmacol **1987**; 23:467–72.
22. Gustafsson LL, Walker O, Alván G, et al. Disposition of chloroquine in man after single intravenous and oral doses. Br J Clin Pharmacol **1983**; 15:471–9.

23. Neuvonen PJ, Kivistö KT, Laine K, Pyykkö K. Prevention of chloroquine absorption by activated charcoal. Hum Exp Toxicol **1992**; 11:117–20.
24. Furst DE. Pharmacokinetics of hydroxychloroquine and chloroquine during treatment of rheumatic diseases. Lupus **1996**; 5(Suppl 1):S11–5.
25. Quintart J, Leroy-Houyet MA, Trouet A, Baudhuin P. Endocytosis and chloroquine accumulation during the cell cycle of hepatoma cells in culture. J Cell Biol **1979**; 82:644–53.
26. Ying C, De Clercq E, Neyts J. Lamivudine, adefovir and tenofovir exhibit long-lasting anti-hepatitis B virus activity in cell culture. J Viral Hepat **2000**; 7:79–83.
27. Abdel-Aziz AK, Shouman S, El-Demerdash E, Elgendy M, Abdel-Naim AB. Chloroquine synergizes sunitinib cytotoxicity via modulating autophagic, apoptotic and angiogenic machineries. Chem Biol Interact **2014**; 217:28–40.
28. Chen L, Liu HG, Liu W, et al. [Analysis of clinical features of 29 patients with 2019 novel coronavirus pneumonia.] Zhonghua Jie He He Hu Xi Za Zhi **2020**; 43:E005.
29. Schrezenmeier E, Dörner T. Mechanisms of action of hydroxychloroquine and chloroquine: implications for rheumatology. Nat Rev Rheumatol **2020**; 16:155–66.
30. Savarino A, Boelaert JR, Cassone A, Majori G, Cauda R. Effects of chloroquine on viral infections: an old drug against today's diseases? Lancet Infect Dis **2003**; 3:722–7.
31. Lianhan S, Jianping Z, Yi H, Du Ronghui, Bin C. On the use of corticosteroids for 2019-nCoV pneumonia. Lancet **2020**; 395:683–4.
32. Strand V, Ahadieh S, French J, et al. Systematic review and meta-analysis of serious infections with tofacitinib and biologic disease-modifying antirheumatic drug treatment in rheumatoid arthritis clinical trials. Arthritis Res Ther **2015**; 17:362.